Chapter 8
Drought Monitoring and Assessment Using Remote Sensing

Z. Su, Y. He, X. Dong, and L. Wang

8.1 Introduction

Drought has wreaked havoc to human societies throughout history. Impacts of drought include devastated crops, famine and conflicts and wars. Serious and severe droughts have occurred on every continent throughout history (Heffernan 2013), including the global mega drought of 4200 years ago that is linked to demise of Akkadian Empire (Kerr 1998) and civilisations in Greece, Egypt and the Indus Valley of Pakistan, the great famine in 1876–1878 which resulted in more than 5 million deaths in India and 30 million in total, the federation drought in 1901 in Australian, the US dust bowl in the 1930s, the central European drought in the 1940s and the Sahel drought in 1970s and 1980s when famine led to 600,000 deaths in 1972–1975, and again in 1984–1985. These droughts have all been associated with climatic shifts that caused low rainfall and as such climate change is now an accepted powerful causal agent in the evolution of civilisation. In many regions, climate change is expected to increase the amount of land at risk from drought and heat and will threaten more arable areas. Timely assessment and monitoring of drought will increase the drought preparedness, relief and mitigation and reduce the damage of drought impacts to the environment, economy and society.

Z. Su, Ph.D. (✉) • L. Wang, M.Sc.
Faculty of Geo-Information Science and Earth Observation (ITC), University of Twente, Hengelosestraat 99, P.O. Box 217, Enschede 7500 AE, The Netherlands
e-mail: z.su@utwente.nl; l.wang-3@utwente.nl

Y. He, Ph.D.
National Meteorological Center, University Road No. 8, Beijing 100081, P.R. China
e-mail: yanbohe@cma.gov.cn

X. Dong, Ph.D.
China Three Gorges University, University Road No. 8, Yichang 443002, Hubei, P.R. China
e-mail: xhdong24@hotmail.com

V. Lakshmi (ed.), *Remote Sensing of Hydrological Extremes*, Springer Remote Sensing/Photogrammetry, DOI 10.1007/978-3-319-43744-6_8

Drought may be defined as the lack of water of a certain location in a certain period compared to a climatic average. From a climatic perspective, we may distinguish meteorological, soil moisture and hydrological drought. Meteorological drought refers to a shortage of precipitation compared to a climatic average; soil moisture drought can be caused by a shortage of precipitation, excessive evaporation and transpiration due to dry weathers and lack of irrigation, while hydrological drought is caused by a combination of lack of precipitation and excessive use of available water resources. When the impact of drought is also taken into consideration, four types of droughts are usually defined such as meteorological drought, agricultural drought, hydrological drought and socioeconomic drought.

As remote sensing provides real-time spatial observations of several atmospheric and land surface variables that can be used to estimate precipitation, evapotranspiration, soil moisture and vegetation conditions, such data can be used for assessment and monitoring of drought characteristics: its intensity, duration and spatial extent. When combined with modelling and forecasting of the water cycle, information on future drought can also be generated for drought preparedness.

In next section, we will briefly review some commonly used drought indices with a focus on the use of remote sensing. A unified framework for drought monitoring and assessment is discussed in Sect. 8.3, and Sect. 8.4 presents several practical examples. Conclusions and recommendations are presented in the last section.

8.2 Drought Indices

Due to the complexity of the drought phenomena and the needs for their descriptions in applications, a panoply of indices has been developed and many recent studies have evaluated their usefulness and consistencies in describing drought events (e.g. Zargar et al. 2011; Eden 2012; van Hoek 2016 among others). In particular, Zargar et al. (2011) reviewed 74 such indices and mentioned that around 150 had been developed in the past. Eden (2012) assessed the droughts in Twente in the Netherlands from 2003 to 2012 by mapping evapotranspiration using the Water Cycle Multi-mission Observation Strategy (WACMOS) methodology (Su et al. 2014) in applying the Surface Energy Balance System (SEBS) (Su 2002). van Hoek (2016) developed a web-based open source platform for global drought monitoring using eight indices (see later for more details).

From a process point of view, meteorological drought occurs when a consistent decline of precipitation reduces water available on land in snow packs, ice sheets, lakes and rivers, therefore a relevant index should primarily describe the decline of precipitation, the Standardised Precipitation Index (SPI) (McKee et al. 1993, 1995; Guttman 1999) can be used for this purpose, although the Palmer Drought Severity

Index (PDSI) (Palmer 1965, 1968) is also widely used but its estimation is more involved than SPI.

Soil moisture drought (or commonly referred to as agricultural drought but this latter gives the impression concerning only agricultural lands and ignoring other natural surfaces) occurs when soil dries out due to evaporation into the atmosphere, drainage into deeper layers that cannot be accessed any more by vegetation or due to excessive human extraction of aquifer storage. The most relevant indices should be those reflecting the soil moisture status in the rooting zone. The PDSI may serve also this purpose. Other relevant indices are the Drought Severity Index (DSI) derived from surface energy balance to infer water balance in the rooting zone (Su et al. 2003a, b) and the Evapotranspiration Deficit Index (ETDI) derived from a hydrological model of the unsaturated zone (Narasimhan and Srinivasan 2005) as well as the Standardised Precipitation and Evaporation Index (SPEI) (Vicente-Serrano et al. 2010a).

Hydrological drought occurs when water reserves in aquifers, lakes and reservoirs fall below averages due to high human demand or low rainfall supplies. The most relevant indices for this should reflect the changes in total storage in an area; the PDSI can be used in part as it considers the accumulation of precipitation, but better is the changes derived from water cycle budget for a certain area which will be described in Sect. 8.3.

From an impact point of view, many remotely sensed indices have been developed in the past decades to describe different aspects of droughts, despite the fact that they mostly reflect the surface conditions instead of the amount of water in the different storages. The following indices are often used: Normalised Difference Vegetation Index (NDVI), Anomaly Vegetation Index, Vegetation Condition Index, Normalised Difference Water Index, Normalised Difference Drought Index and Vegetation Supplication Water Index based on visible, near infrared, shortwave reflectance data for partly and fully covered surface, Temperature Vegetation Dryness Index, Temperature Condition Index, Crop Water Stress Index and Water Deficit Index based on thermal infrared remote sensing data for partly and fully covered surface. A detailed review of these indices can be found in McVicar and Jupp (1998).

In the following, we briefly review some commonly used drought indices focusing on the use of remote sensing as well as reanalysis type of gridded data that use remote sensing data as input or assimilate such data as state variables.

8.2.1 PDSI

The procedure to estimate PDSI is as follows: (1) Carry out a hydrologic accounting by months for a long series of years. (2) Summarise the results to obtain certain constants or coefficients which are dependent on the climate of the area being analysed. (3) Reanalyse the series using the derived coefficients to determine the amount of moisture required for "normal" weather during each month. (4) Convert

the departures to indices of moisture anomaly. (5) Analyse the index series to develop: (a) Criteria for determining the beginning and ending of drought periods. (b) A formula for determining drought severity.

As the estimation of PDSI relies on a hydrological accounting, the challenges in using this approach are in the definition of the two soil layers with the corresponding field capacity which requires some knowledge of soil hydraulic properties and the estimation of the potential recharge, loss, precipitation, evaporation and runoff as well as the associated coefficients (i.e. evapotranspiration, recharge, runoff, and loss). A comprehensive land surface hydrological modelling may easily accomplish this task given adequate forcings.

8.2.2 SPI

SPI (McKee et al. 1993) is based only on precipitation data, thus provides a rapid drought index once precipitation data is available. SPI compares precipitation with its climatic mean estimated as multiyear average. To estimate SPI, the precipitation record is first fitted to a gamma distribution, which is then transformed into a normal distribution using an equal probability transformation. After standardisation, i.e. $\mathrm{SPI} = (X_i - m[X])/\mathrm{std}[X]$, where X_i is the precipitation variable, $m[X]$ the average (typically over a period of 30 years) and $\mathrm{std}[X]$ the standard deviation, SPI values above zero indicate wet periods and values below zero indicate dry periods.

For any given event, its SPI score represents how many standard deviations its cumulative precipitation deficit deviates from the normalised average. If a value of less than zero is consistently observed and it reaches a value of -1 or less, a drought is said to have occurred (McKee et al. 1993), thus the onset of a drought can be defined. SPI can be calculated for different time periods, but typically it is applied for the 3, 6, 12, 24 and 48-month periods. Because over time precipitation deficit gradually and variably affects different water resources (e.g. snowpack, stream flow and groundwater), the multitude of SPI durations can be used to reflect change in different drought features.

8.2.3 NDVI, VCI, TCI and VHI

NDVI (Kriegler et al. 1969; Rouse et al. 1973; Tucker 1979) has been used as a surrogate for detecting the condition of green vegetation, as it is defined as $\mathrm{NDVI} = (\mathrm{NIR} - \mathrm{VIS})/(\mathrm{NIR} + \mathrm{VIS})$, where VIS and NIR stand for the spectral reflectance measurements acquired in the visible (red) and near-infrared regions of the spectrum. Because the pigment in plant leaves (chlorophyll) strongly absorbs visible light (from 0.4 to 0.7 μm) for use in photosynthesis and the cell structure of the leaves strongly reflects near-infrared light (from 0.7 to 1.1 μm), the more green

leaves a plant has, the more these wavelengths of light are affected, respectively, and hence the higher the NDVI. As such NDVI has also been used for detecting drought effects on vegetation and used as a base index for a number of remote sensing indices that similarly measure vegetation conditions.

Among these the most popular ones are the Vegetation Condition Index (VCI) (Kogan 1990), defined as $VCI = (NDVI - NDVI_{min})/(NDVI_{max} - NDVI_{min})$ for a certain period (week/month), NDVI is the NDVI for the period under study, $NDVI_{max}$ and $NDVI_{min}$ are the maximum and minimum NDVIs, respectively, in the record for the specific period; and the Temperature Condition Index (TCI) (Kogan 1995), defined as $TCI = (BT_{max} - BT)/(BT_{max} - BT_{min})$ which describes the deviation of the brightness temperature (BT) in a period (e.g. a month) from recorded maximum assuming the higher the temperature deviation, the higher the drought. BT, BT_{max} and BT_{min} are the actual, maximum and minimum BTs, respectively, in the record for the specific period. Combining the VCI and TCI using a weight factor α for the contributions of VCI and TCI, the Vegetation Health Index (VHI) (Kogan 1995) can be defined as $VHI = \alpha VCI + (1 - \alpha)TCI$ and often α is set to 0.5 and is found more effective than other vegetative drought indices (Kogan 2001).

By replacing the respective minimum or maximum values in the definition of VCI, TCI with the mean values and make proper adjustment in the equations, Jia et al. (2012) defined the Normalised Vegetation Anomaly Index (NVCI), the Normalised Temperature Anomaly Index (NTCI) and the Normalised Drought Anomaly Index (NDAI), respectively, as, $NVAI = (NDVI - m[NDVI])/(NDVI_{max} - NDVI_{min})$, $NTAI = (BT - m[BT])/(BT_{max} - BT_{min})$, $NDAI = \alpha NVCI - (1 - \alpha) NTAI$, where $m[.]$ is the respectively corresponding mean value.

van Hoek (2016) has evaluated these indices with ground observations in China and concluded that the normalised values to be more stable than the original indices, while also pointing out difficulties to validate the satellite-derived drought maps with the national hazard database of China Meteorological Administration.

8.2.4 DSI, ETDI and SPEI

The Drought Severity Index (DSI) (Su et al. 2003a) was developed to infer rooting zone soil moisture from surface energy balance consideration. By considering only the vertical movement of water, which is a valid approximation in the absence of heavy rainfall and irrigation and under deep groundwater conditions, it is possible to derive a physical relationship between the temporal changes of the evaporation and the changes of the soil water content. Using the mass conservation principle for an infinitesimal soil layer in the vertical direction, we obtain

$$\frac{\partial \theta(z,t)}{\partial t} = -\frac{\partial q(z,t)}{\partial z} \tag{8.1}$$

where θ, q, t, z are volumetric soil moisture content, soil water flux density (water amount per unit area per unit time) across a vertical plane, time and vertical distance increment, respectively. Integrating (8.1) from z_1 to z_2 in depth and from t_1 to t_2 in time and assuming that there is no source/sink between z_1 and z_2, we obtain the water balance equation,

$$\int_{z_1}^{z_2} \theta(z,t_2)\mathrm{d}z - \int_{z_1}^{z_2} \theta(z,t_1)\mathrm{d}z = Q(z_1) - Q(z_2) \tag{8.2}$$

Applying (8.2) to the active rooting zone with the boundary conditions $Q(z_1) = P_0 + I_0 - E$ at the soil surface and $Q(z_2) = I_c$ at the bottom of the rooting zone, the change of total soil water content in this zone can be written as

$$\Theta(t_2) - \Theta(t_1) = P_0 + I_0 + I_c - E \tag{8.3}$$

where Θ is the volumetric soil water content in the rooting zone, P_0, I_0, I_c, E are, respectively, precipitation, irrigation, capillary flux and evapotranspiration amount from t_1 to t_2.

Similar to the determination of relative evaporation as used in SEBS (Su 2002), the water balance at limiting cases can be considered. Without losing generality, we assume that the soil in the rooting zone was completely saturated at t_1, i.e. $\Theta(t_1) = \Theta_{wet}$ (i.e. at the wet limit) after a sufficient precipitation or irrigation event. During the drying-down process (i.e. there is no precipitation or irrigation taking place during this period), the rooting zone will eventually reach the dry limit $\Theta(t_2) = \Theta_{dry}$, i.e. the evaporation becomes zero due to the limitation of the soil moisture (which drops to below the wilting point), from (8.3) we have,

$$\Theta_{wet} - \Theta_{dry} = I_{c,wet} - E_{wet} \tag{8.4}$$

Similarly, for any time between the wet-limit and the dry-limit cases, we obtain from (8.3)

$$\Theta - \Theta_{dry} = I_c - E \tag{8.5}$$

Manipulating (8.4) and (8.5) results in

$$\frac{\Theta - \Theta_{dry}}{\Theta_{wet} - \Theta_{dry}} = \frac{E - I_c}{E_{wet} - I_{c,wet}} \tag{8.6}$$

Assuming the capillary flux is only related to soil texture and is small compared to root water uptake which can be quantified by the transpiration flux, i.e. $I_c = I_{c,wet} << E$ as observed by Aydin (1994) who reported that the capillary

flux was very small when compared with root water uptake, even in clay soils. Subsequently by defining $R_\theta = \Theta/\Theta_{\text{wet}}$ as the relative soil water content with respect to the porosity and using (8.6) (and multiplying the right-hand side by λ, the latent heat of vaporisation), we arrive at

$$R_\theta = \frac{\Theta}{\Theta_{\text{wet}}} = \frac{\lambda E}{\lambda E_{\text{wet}}} \tag{8.7}$$

Equation (8.7) shows that the relative soil water content is directly related to the relative evapotranspiration. As such if defining the Drought Severity Index as $\text{DSI} = 1 - R_\theta$, i.e. the relative soil water deficit in the rooting zone, one obtains from the SEBS relationship (Su 2002),

$$\text{DSI} = \frac{H - H_{\text{wet}}}{H_{\text{dry}} - H_{\text{wet}}} \tag{8.8}$$

Equation (8.8) is the required quantitative measure for soil water deficit in the rooting depth and can be directly derived from SEBS calculation (Su 2002). When DSI is high, soil water content is low and vice versa.

By relating DSI to soil hydraulic characteristics (i.e. the porosity) and to crop phenology (i.e. the rooting depth), location-specific soil water deficit in the rooting zone can be determined for a particular soil, thus leading to a quantitative assessment of drought severity for the concerned crop at the particular location and time. This can be done as follows by defining the relative evapotranspiration as in SEBS (Su 2002) and linking it to (8.6) as

$$\text{DSI} = 1 - \Lambda_{\text{r}} = 1 - s\left(\frac{\Theta - \Theta_{\text{dry}}}{\Theta_{\text{wet}} - \Theta_{\text{dry}}}\right) \tag{8.9}$$

A general form with a sigmoid function, $y = \frac{1}{1+e^{-x^a}}$, can then be fitted to the soil moisture function $s(.)$ to account for the local soil properties. By relating the factor a (the exponent) to different soil hydraulic properties all conditions can be taken into account as shown in Fig. 8.1.

8.2.5 *Case Studies*

The Evapotranspiration Deficit Index (ETDI) was defined (Narasimhan and Srinivasan 2005) by using simulated data with the SWAT model (Arnold et al. 1998; Neitsch et al. 2002). The water stress anomaly (WSA) is calculated as case A: if $\text{WS}_{i,j} <= \text{MWS}_j$, then $\text{WSA}_{i,j} = (\text{MWS}_j - \text{WS}_{i,j})/(\text{MWS}_j - \text{minWS}_j)$ *100, or case B: If $\text{WS}_{i,j} > \text{MWS}_j$, then $\text{WSA}_{i,j} = (\text{MWS}_j - \text{WS}_{i,j})/(\text{maxMWS}_j - \text{NWS}_j)$*100 (Note: it was specified in Narasimhan and Srinivasan

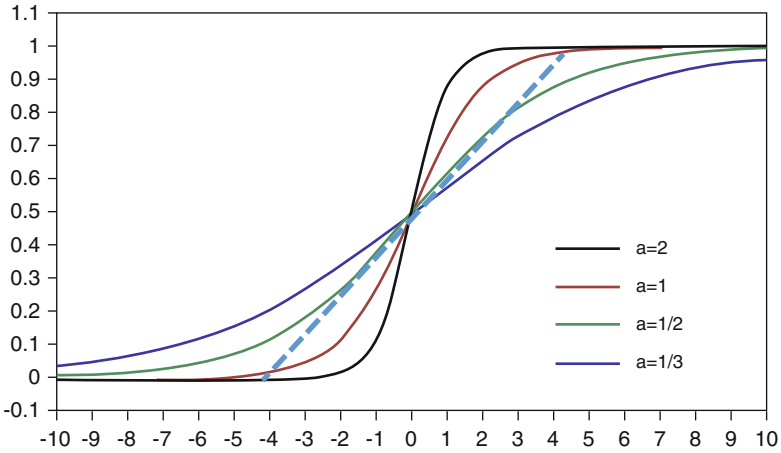

Fig. 8.1 Generalised form $y = \frac{1}{1+e^{-x^a}}$ between relative evaporation (y, ordinate) and normalised soil moisture (x, abscissa), the factor a (the exponent) can be used to fit different soil properties. The *dashed line* indicates the simple linear relationship of (8.7)

2005 that A holds for $WS_{i,j} = MWS_j$, but this is likely a typo, as it would make no difference for A or B if $WS_{i,j} = MWS_j$), and in these expressions, WSA is the weekly water stress anomaly, MWS_j is the long-term median water stress of week j, $MaxWS_j$, $MinWS_j$ are the long-term maximum and minimum water stress of week j, and WS is the weekly water stress ratio, defined as $WS = (ET_0 - ET)/ET_0$, where ET_0 is the weekly reference crop evapotranspiration, and ET is the weekly actual transpiration. Eden (2012) evaluated the usefulness of ETDI for regional drought analysis and compared it to SPI from a meteorological station operated by the Royal Meteorological Institute of the Netherlands (KNMI) from 2003 to 2010 and concluded that the ETDI can be used to estimate the onset, intensity and duration of spatially regional drought.

The Standardised Precipitation Evapotranspiration Index (SPEI) (Vicente-Serrano et al. 2010a) is defined using precipitation and potential evapotranspiration (PET) similar to the PDSI. First, the climatic water balance, i.e. the difference between precipitation and ET_0, is estimated as:

$$D = P - ET_0 \tag{8.10}$$

where P is the monthly precipitation (mm) and ET_0 (mm) is estimated with the method of Thornthwaite (1948), using only mean monthly temperature and the geographical location of the region of interest. Then the calculated D values were aggregated at various time scales:

$$D_n^k = \sum_{i=0}^{k-1} (P_{n-i} - ET_{n-i}), \quad n \geq k \tag{8.11}$$

where k (months) is the time scale of the aggregation and n is the calculation number. The D values are undefined for $k > n$. Finally a log-logistic probability distribution function was then fitted to the data series of D, as it adapts very well to all time scales (Vicente-Serrano et al. 2010b).

The SPEI combines the sensitivity of the PDSI to changes in evaporation demand (caused by temperature fluctuations and trends) with the multitemporal nature of the SPI and the main advantage of the new index lies in its multiscalar character, which allows discrimination between different types of drought.

Different time scales are needed for monitoring drought conditions in different hydrological subsystems, as short time scales are mainly related to soil water content and river discharge in headwater areas, medium time scales to reservoir storages and discharge in the medium course of the rivers, and long time scales to variations in groundwater storage. For regional drought assessment and mitigation, spatial data of high resolution (i.e. kilometre scale or field scale) will be of great benefit; therefore, in next section we propose a unified framework for multiscale temporal and spatial drought assessment, monitoring and analysis as well as prediction.

8.3 A Unified Framework for Drought Monitoring and Assessment

As discussed in Sect. 8.2, many indices have been proposed for drought assessment, each of these indices addresses a specific aspect of drought. It is therefore desirable to have one or a set of consistent indices to describe all aspects of a drought, its onset, severity and duration, as well as their spatial distribution and simultaneously addressing meteorological, soil moisture and hydrological drought. Recently, van Hoek (2016) has evaluated different indices and proposed the use of eight indices for drought monitoring in China in a web-GIS-based system. The used indices are as follows: Precipitation Anomaly Percentage (PAP), TCI, NTAI, VCI, NVAI, VHI, NDAI and the Evapotranspiration Deficit Index (EDI).

On the basis of the review presented in Sect. 8.2 and the studies by Eden (2012) and van Hoek (2016), a drought monitoring and analysis system should take into account the meteorological, soil moisture as well as hydrological characteristics, thus a system using SPI, DSI-ETDI, SPEI and VCI should be able to describe surface characteristics of droughts (i.e. meteorological and soil moisture drought), and as for hydrological drought a water cycle closure (or the simplified water budget closure for a catchment) approach (Fig. 8.2) is then needed.

In order to be able to compare these indices, the same standardisation procedure can be used for other indices and variables providing a uniform descriptor for different aspects of the same event. We shall name this index as: $\mathrm{SXI} = (X_i - m[X])/\mathrm{std}[X]$, where X_i is the variable in question and $m[X]$ is the average (typically over a period of 30 years), std[X] is the standard deviation, and when X is replaced by a certain variable we derive a specific index for that variable (e.g. precipitation,

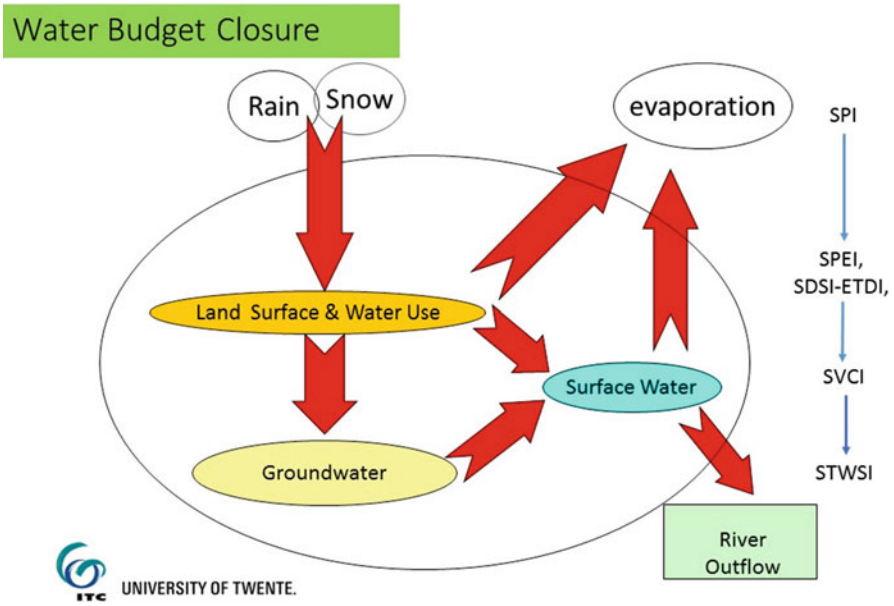

Fig. 8.2 Concept of water budget closure. *SPI* is the Standardised Precipitation Index, *SPEI* is standardised Precipitation Evaporation Index, *SDSI-ETDI* is the Standardised Drought Severity Index-Evapotranspiration Deficit Index, *SVCI* is Standardised Vegetation Condition Index, *STWSI* is the Standardised Terrestrial Water Storage Index, all calculated on weekly or monthly time interval from 1 to *N* time intervals (e.g. for 48 months) (i.e. as anomalies and cumulative anomalies)

evaporation/transpiration, soil moisture, vegetation condition, etc.). As such this SXI is defined in the same manner as standardised anomaly and will be used interchangeably.

For water budget closure of a catchment, the following equation can be used,

$$\frac{\partial S_{i,j}}{\partial t} = P_{i,j} - E_{i,j} - R_{\text{Obs}} * f\left(P_{i,j}, E_{i,j}\right) \tag{8.11}$$

The left-hand side of the equation represents the change of total water storage and the right-hand side states that the total water storage change equals to precipitation less evaporation and discharge. The function $f(.)$ is used to scale the aggregated discharge at the gauge station to runoff generation at each grid.

In the calculation to be presented in Sect. 8.4, the precipitation is from satellite observation (e.g. Adler et al. 2003), the evaporation is calculated by SEBS (Su 2002; Chen et al. 2014) and the discharge is from in situ observation. This equation also expresses the consistency validation among in situ observation datasets, thus different datasets for precipitation, evaporation and runoff can be used and their consistency evaluated.

In addition to satellite and in situ observation datasets, reanalysis data, e.g. the ERA-Interim, provide these three variables as well, so ERA-interim results will be

applied with this equation to calculate the total water storage change as well. On the other hand, the total water storage can be measured by using the GRACE satellite, thus these different data sources can be assessed in one consistent framework.

A set of sequential standardised indices can then be used to describe the different aspects of droughts, SPI for precipitation, SPEI for precipitation and potential evaporation and SDSI-ETDI for evapotranspiration, SVCI for vegetation condition and STWSI for the terrestrial water storage in the catchment, all calculated on weekly or monthly time interval from 1 to N time intervals (e.g. for 48 months) (i.e. as standardised anomalies and cumulative anomalies) (Fig. 8.2).

For the determination of the drought intensity, a similarly uniform approach could be proposed for the different indices, and as they are standardised a normal distribution can be fitted to them (or after some transformation), as such it is sufficient to use the standard deviation of the indices to define their departure from the mean. The corresponding drought intensity classes are listed in Table 8.1.

The utilities of these indices and definitions will be illustrated with some practical examples in next section as executed in the Dragon drought monitoring project supported by the European Space Agency and the Ministry of Science and Technology of China.

8.4 Drought Monitoring and Prediction over Continental China: A Case Study

The conflict between supply and demand of water resources constitutes the biggest problem for food security of an increasing world population. Since 1970s, some progresses have been made in drought quantification and research. However, the methods employed are mostly based on data collected on local meteorological variables and cannot quantify real-time, large-scale actual drought process, i.e. its intensity, duration and its actual extent. It has also often happened that a drought is not recognised while it is in fact already underway of its development. As a result of this inability, no adequate measure can be deployed to effectively fight any big drought disaster often causing great hunger and social instability. Most recently, China Meteorological Administration has installed nation-wide automatic soil moisture monitoring stations providing important in situ observation of the status of soil moisture, such that information derived from spatial remote sensing data can be validated and improved for real-time drought monitoring.

8.4.1 Satellite Earth Observation of Land Surface Processes

The project strategy is to derive land surface parameters and heat fluxes using satellite earth observation techniques and to apply these parameters and fluxes in a hydrometeorological model as initial conditions and constraints at the

Table 8.1 Drought intensity defined as departure from the mean (i.e. number of standard deviations), the suggested category and the return period in number of intervals (e.g. once in how many years) as well as the suggested colour scheme for maps

Value range	Category	Return period (1 in …)
$F <= \mu - 3\sigma$	Extremely dry	15787
$\mu - 3\sigma < F <= \mu - 2\sigma$	Severely dry	370
$\mu - 2\sigma < F <= \mu - 1\sigma$	Moderately dry	22
$\mu - 1\sigma < F < \mu + 1\sigma$	Near normal	3
$\mu + 1\sigma <= F < \mu + 2\sigma$	Moderately wet	22
$\mu + 2\sigma <= F < \mu + 3\sigma$	Severely wet	370
$\mu + 3\sigma <= F$	Extremely wet	15787

land–atmosphere interface. Further data assimilation allows controlling the model drifts. Since a hydrological model treats, in reality, heterogeneous land surfaces by means of effective parameters, and there is no any other adequate means, except satellite earth observation techniques, to derive the actual distribution of these parameters over any large area, this proposed strategy makes a major progress to monitor and predict drought on a quantitative way. It is also well known that both type of models treat soil water content, which controls the energy and water partition at the land–atmosphere interface, as a prognostic variable or put it plainly as a residual of the mass balance equation. Any prediction of soil water content using these models, without other actual physical information, is simply a collection of residual errors of other terms and does not provide any reliable indication of the actual soil water content. The latter as a matter of fact is the most important variable sorted after for drought problems. On the other hand, since satellite earth observation provides actual measurements of land surface parameters and models enable to make predictions, it becomes fairly clear that only a combined approach will provide the definitive opportunities to adequately solve the drought problem over a large area.

Radiometric observations aboard earth observation satellites are an attractive source of spatial observations of land surface processes and can be used to determine the required model parameters. In the Dragon drought monitoring project, we have considered the following variables: sensible and latent heat fluxes; evaporative fraction and actual evaporation; and root zone soil water content index, all important to hydrological modelling. Different satellite data were used to derive land surface physical variables as given by Su (2001).

The state-of-the-art remote sensing algorithm package SEBS (Surface Energy Balance System) (Su 2001, 2002) for mapping heat fluxes for heterogeneous land surfaces was used to derive sensible and latent heat fluxes. The main input data to SEBS are satellite images and meteorological variables. Spatial inputs to SEBS are land surface parameters such as incoming global radiation, albedo, vegetation index for fractional coverage and roughness determination, surface temperature, emissivity and roughness length due to both topography and vegetation effects. The advantage of the system is that no a priori knowledge of heat fluxes is required and no site-specific calibration is needed. Data of high or low spatial resolution from all sensors in the visible, near-infrared and thermal infrared frequency ranges can be used in the system.

After obtaining the sensible and latent heat fluxes, the evaporative fraction (EF) can be calculated as the ratio of the latent heat flux to the total available energy. Further, by making the assumption that the derived evaporative fraction represents the daily average, the actual evaporation can be calculated with an estimate of daily net radiation (Su 2001; Li 2001).

Since it has been demonstrated that EF is often conservative during daytime, and from its definition given earlier (see Sect. 8.2), it represents physically the amount of energy used for evaporation during daytime. As it has long been established that evaporation is strongly regulated by soil water availability under the same atmospheric forcing, i.e. from potential when the soil is saturated to nearly zero when it dries out, EF can be used to quantify the soil water availability. Compared to

surface soil moisture as can be determined using both active microwave and passive microwave techniques (e.g. Su et al. 1997), use of EF gives a good indication of the water availability in the whole rooting zone.

Because of cloud contamination and missing data in satellite data, the derived land surface parameters will contain missing values and gaps causing undesirable uncertainty in drought monitoring and prediction. The Harmonic Analysis of Time Series (HANTS) algorithm (Verhoef 2000) can be used to replace the wrong or missing data. The advantages of HANTS include: (a) screening and removing cloud-affected observations; (b) temporal interpolation of remaining observations to reconstruct images at any prescribed time. Roerink et al. (2000) have demonstrated the capability of HANTS in reconstructing cloud-free vegetation index images. Using HANTS reconstructed monthly evaporative fraction and surface albedo in combination with observed monthly global radiation provided by meteorological stations, it has been shown that this strategy is successful in deriving monthly actual evaporation in Northwest China (Li 2001).

8.4.2 Hydrometeorological Modelling

Ideally a large-scale hydrological model should be operated for real-time tracking of water budget and such a model should include precipitation, snow melt, evaporation/transpiration, surface runoff, unsaturated flow and groundwater flow, flow routing, reservoir and lakes regulation. When the model is embedded in a GIS (Geographic Information System) environment and operated on a predefined grid scale, a better compatibility can be achieved with both satellite earth observation products and the atmospheric models, for prediction purposes.

As large hydrometeorological fields are generated by ECMWF (European Centre for Medium-range Weather Forecast) Integrated Forecast System over global scale as well as the global data assimilation system for land (GLDAS) operated by the National Aeronautics and Space Administration (NASA), they can be converted into standardised indices or anomalies for drought analysis. The reliability of the modelling and prediction for China can be established by comparing historical predictions, especially for drought prone areas, to national statistics. Surface observations of precipitation from the meteorological networks in China (around 600 stations) are used to validate and update the consistency of the different fields.

In the following, we show some analyses conducted for several river basins and for the whole China when its southwest region suffered a heavy drought lasting for several months in 2010.

To do so, the country is divided into various river basins by means of a digital elevation model in the Integrated Land and Water Information System (ILWIS) (https://www.itc.nl/Pub/research_programme/Research-review-and-output/ILWIS_-_Remote_Sensing_and_GIS_software.html) (Fig. 8.3).

Then the calculations are done as follows for each river basin using the standardised indices.

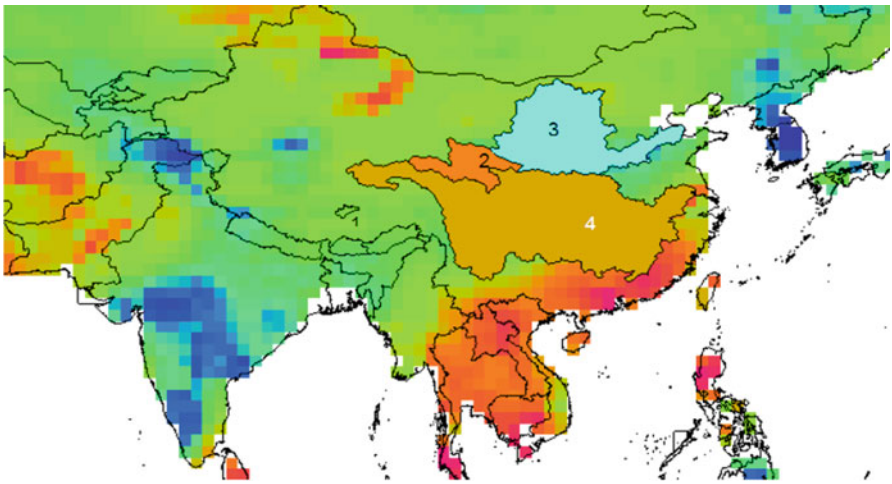

Fig. 8.3 River basins delineated in a GIS system, No. 1—Namco basin, No. 2—The upper Yellow River Basin, No. 3—the whole Yellow River Basin (incl. the upper part), No. 4—the Yangtze river basin

- GLDAS_STWS2I: GLDAS-derived Standardised total water storage index, generated by the following equation:

  GLDAS_STWS2I = ΔTWS2/GLDAS_TWS2 (std)
  GLDAS_TWS2 = $P - \mathrm{ET} - R$
  GLDAS_TWS2: GLDAS-derived total water storage of a specific month and year
  GLDAS_TWS2(mean) = mean long-term GLDAS_TWS2 of a specific month
  ΔTWS2 = GLDAS_TWS2 − GLDAS_TWS2(mean)
  GLDAS_TWS2 (std) = standard deviation of long-term GLDAS_TWS2 of a specific month

- TRMM_SPI

  The Standardised precipitation index from TRMM
  SPI = $(P - P(\mathrm{mean}))/P(\mathrm{std})$
  P = precipitation of a specific month and year
  P(mean) = mean long-term precipitation of a specific month
  P(std) = standard deviation of long-term precipitation of a specific month

- GLDAS_SRI

  The Standardised runoff index from GLDAS
  SRI = $(R - R(\mathrm{mean}))/R(\mathrm{std})$
  R = GLDAS-derived runoff of a specific month and year
  R(mean) = mean long-term GLDAS-derived runoff of a specific month
  R(std) = standard deviation of long-term runoff of a specific month

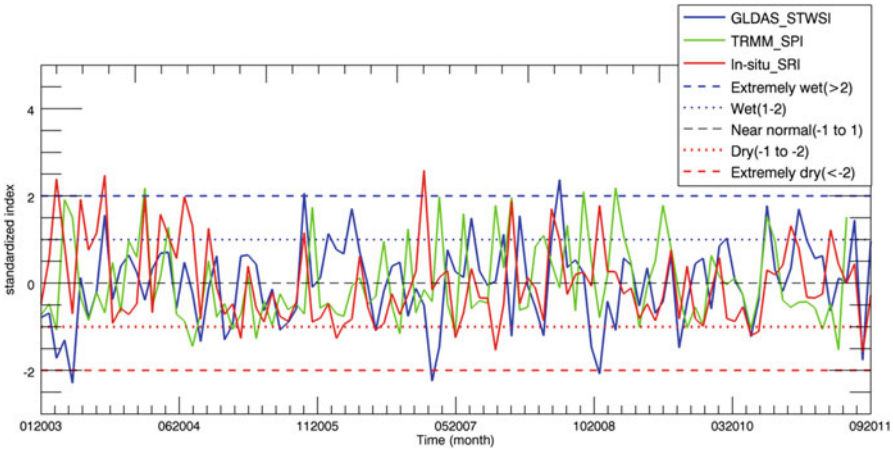

Fig. 8.4 Standardised index in Namco basin (*Note*: the definition of drought categories here follows those by CMA and differs from Table 8.1 in that only severely situations (beyond two standard deviations) were observed but indicated as extremely situations for consistency)

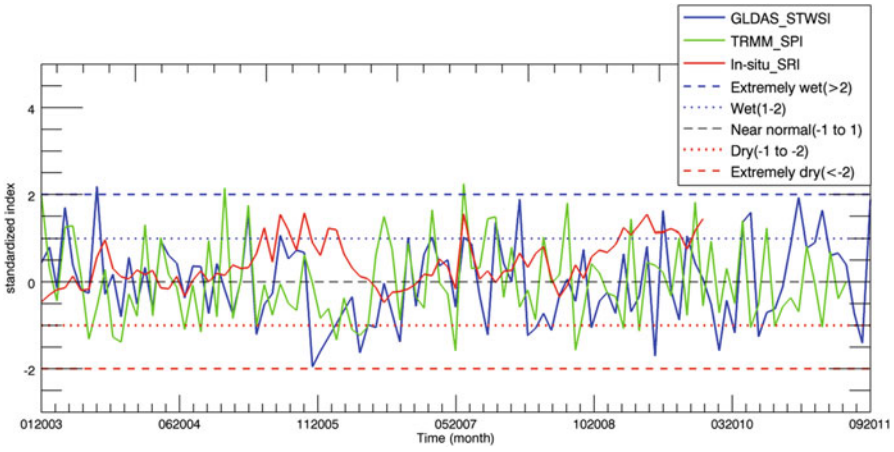

Fig. 8.5 Standardised index in upper Yellow river basin

As the observed runoff is only available for upper yellow river basin, GLDAS-derived runoff is used for TWS2 calculation.

Figures 8.4, 8.5, 8.6 and 8.7 show the calculated indices for the four river basins, and by comparing them to the drought categories, specific drought situation in the basin can be identified.

In Fig. 8.8, we show the Standardised Terrestrial Water Storage Index derived from GLDAS simulation which is generated as follows:

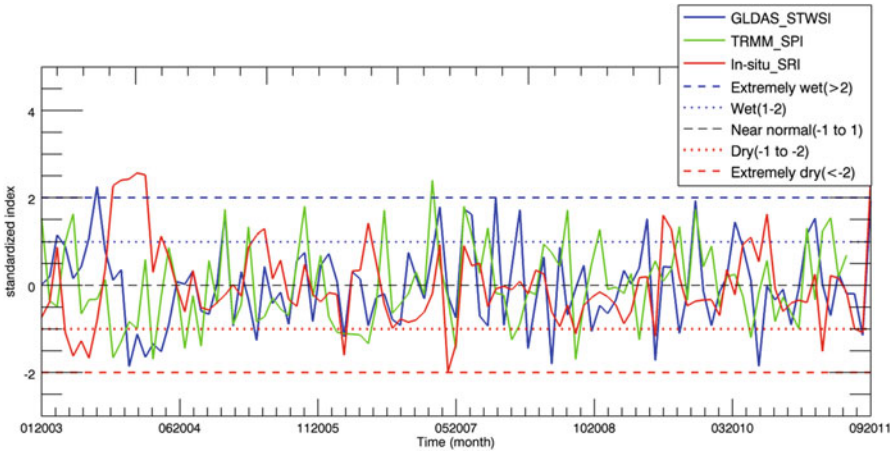

Fig. 8.6 Standardised index in whole Yellow river basin

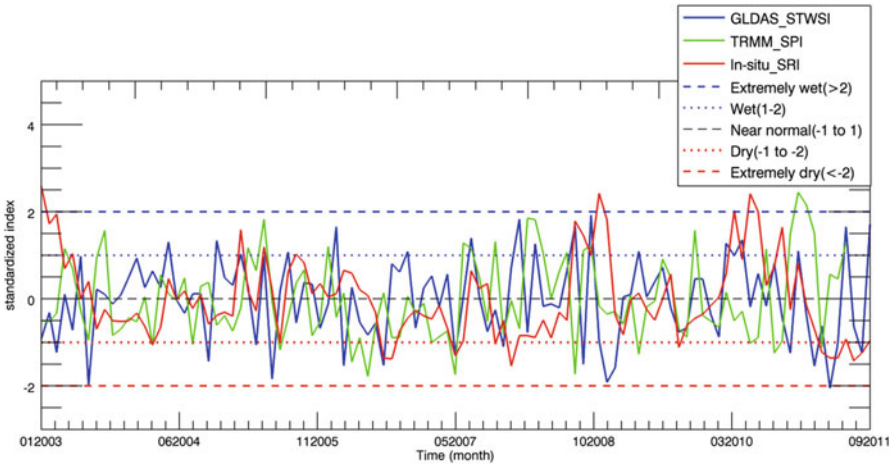

Fig. 8.7 Standardised index in Yangtze basin

GLDAS_STWS1I = ΔTWS1/std(GLDAS_TWS1)
GLDAS-derived total water storage of a specific month and year is given as:

GLDAS_TWS1 = SM + SWE + CWS
mean(GLDAS_TWS1) = mean of long-term GLDAS_TWS1 of a specific month
ΔTWS1 = GLDAS_TWS1 − mean(GLDAS_TWS1)
std(GLDAS_TWS1) = standard deviation of long-term GLDAS_TWS1 of a specific month

Figure 8.8 shows that the drought affected areas in southwest China persisted from January till June 2010 and affected large area with extremely dry conditions.

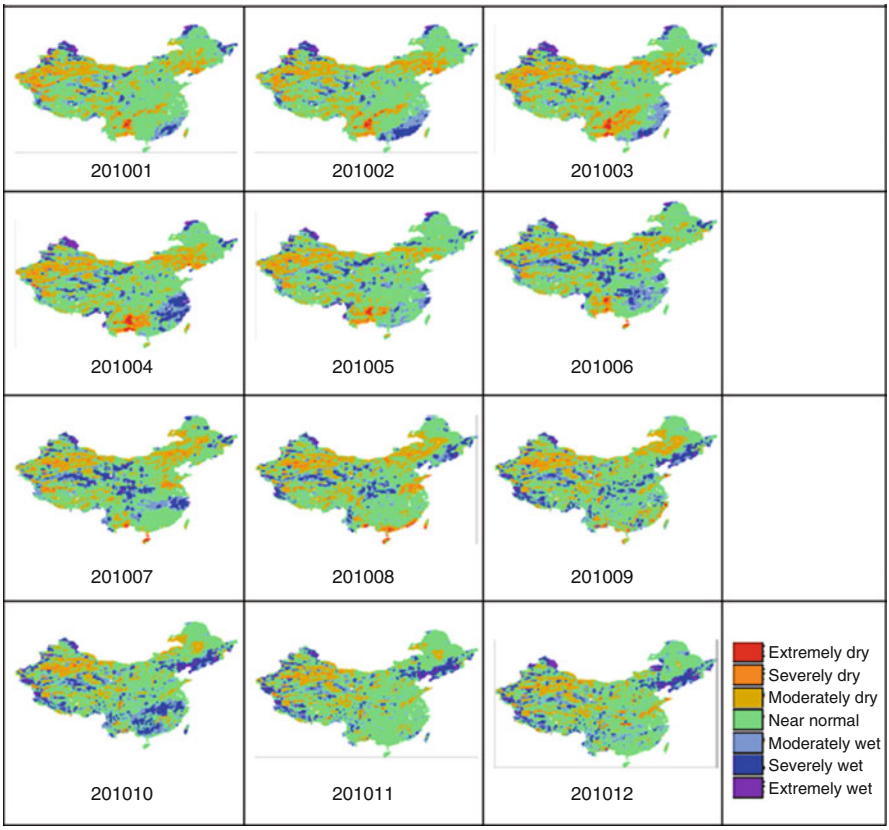

Fig. 8.8 GLDAS-derived Standardised terrestrial water storage index expressed in drought intensity as defined in Table 8.1

To further show the complex character of the drought phenomenon, we display in Fig. 8.9 the spatial drought severity maps derived for southwest China and compare them to in situ observation of soil moisture and drought reports.

The challenges in interpreting these maps and comparing them to both soil moisture observation and drought reports are very obvious. From the satellite-derived SEBS-DSI values, it can be concluded that the regional spatiotemporal variability is very big within the studied region in southwest China. The drought in northwest of Chengdu appeared most severe and persistent for months from beginning of January till beginning of May, but unfortunately there are no in situ soil moisture observations, nor drought reports available. Near Chongqing, the in situ soil moisture stations report large wet conditions, while SEBS-DSI have often missing values due to cloud contamination, but implicitly the consistency of the two datasets is confirmed. Near Guiyang, the information provided by in situ soil moisture observation and drought reports are not consistent while droughts are reported for all the months, the soil moisture observations indicate wetter

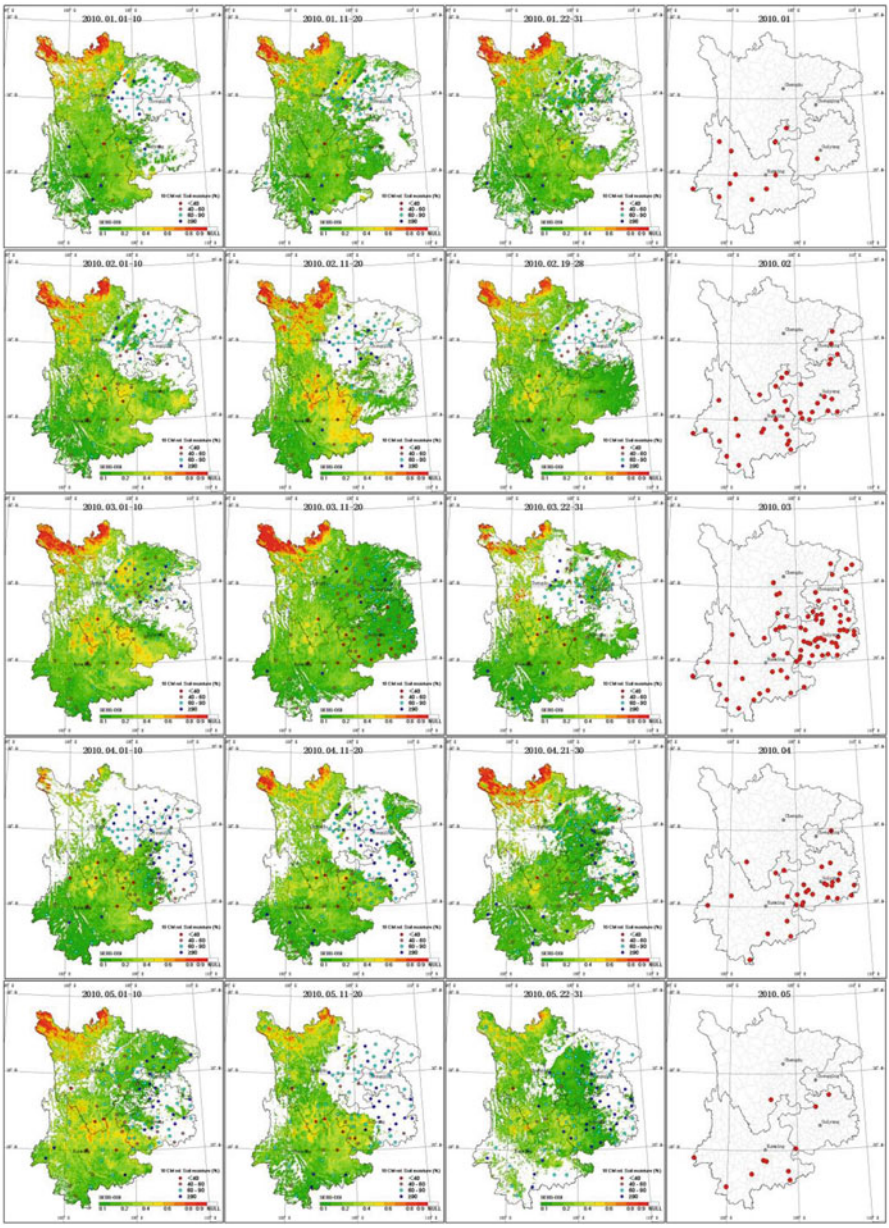

Fig. 8.9 SEBS-DSI with measured 10 cm relative soil moisture overlaid and reported drought situation, January–May 2010 (*from left to right*: first, second, third decade and reported droughts)

conditions. Ideally the SEBS-DSI should be compared to in situ soil moisture observations to establish the accuracy of the calculations, but the real challenges lay in the very local nature of the in situ observations where both very dry and very wet observations are reported within short distance of each other, which may be

influenced by local agricultural practices. Nevertheless and broadly higher SEBS-DSI values correspond to drier soil moisture conditions and the global patterns are consistent. Future analysis should focus on stratification of SEBS-DSI and in situ soil moisture observation per land use (e.g. using NDVI information) and soil textures.

8.5 Summary and Conclusions

Drought phenomenon is very complex as it is caused by a multitude of factors starting from the deficit of precipitation when compared to climatic mean. Such a deficit, when combined with sustained dry weather conditions entertain high evaporation and transpiration and thus result in soil moisture drought if there is no adequate irrigation. Finally, hydrological drought emerges by a combination of lack of precipitation and excessive use of available water resources for a sustained period. To assess historical droughts and to provide drought monitoring, various indices have been proposed for different purposes and using different datasets. Despite the panoply of these indices, when one focuses on the processes that caused droughts, a set of consistent indices may adequately describe the different aspects of the droughts. We propose the use of standardised index, such as SPI for precipitation, SPEI for precipitation and potential evaporation and SDSI-ETDI for evapotranspiration, SVCI for vegetation condition and STWSI for the terrestrial water storage in the catchment, all calculated on weekly or monthly time interval from 1 to *N* time intervals (e.g. for 48 months) (i.e. as standardised anomalies and cumulative anomalies). As remote sensing and hydrometeorological data assimilation systems routinely provide data to derive the different indices, use of them can provide a uniform framework for drought assessment, monitoring and analysis as well as predictions.

Acknowledgements This work is supported in part by the ESA-MOST Dragon programme. We thank them for providing continuous supports in the project in terms of data, financial and logistic supports. We are grateful to colleagues for their supports to the various project activities. This project is conducted in collaboration with the EU FP7 CEOP-AEGIS and CORE-CLIMAX projects.

References

Adler RF, Huffman GJ, Chang A, Ferraro R, Xie P, Janowiak J, Arkin P (2003) The version 2 Global Precipitation Climatology Project (GPCP) monthly precipitation analysis. J Hydrometeorol 4:1147–1167

Arnold JG, Srinivasan R, Muttiah RS, Williams JR (1998) Large area hydrologic modelling and assessment. Part 1. Model development. J Am Soc Water Res Assoc 34(1):73–89

Aydin M (1994) Hydraulic properties and water balance of a clay soil cropped with cotton. Irrig Sci 15:17–23

Chen X, Su Z, Ma Y, Liu S, Yu Q, Xu Z (2014) Development of a 10-year (2001–2010) 0.1-degree dataset of land-surface energy balance for mainland China. Atmos Chem Phys 14 (23):13097–13117

Eden U (2012) Drought assessment by evapotranspiration mapping in Twente, the Netherlands. M. Sc. thesis, Faculty of Geo-Information Science and Earth Observation, (ITC), University of Twente, p 79

Guttman NB (1999) Accepting the standardized precipitation index: a calculation algorithm. J Am Water Resour Assoc 35(2):311–322

Heffernan O (2013) The dry facts. Nature 501(7468):S2–S3

Jia L, Hu G, Zhou J, Menenti M (2012) Assessing the sensitivity of two new indicators of vegetation response to water availability for drought monitoring. Paper presented at the SPIE Asia-Pacific Remote Sens. doi:10.1117/12.977416

Kerr RA (1998) Sea-floor dust shows drought felled Akkadian empire. Science 279 (5349):325–326

Kogan FN (1990) Remote sensing of weather impacts on vegetation in non-homogeneous areas. Int J Remote Sens 11(8):1405–1419

Kogan FN (1995) Application of vegetation index and brightness temperature for drought detection. Adv Space Res 15(11):91–100

Kogan FN (2001) Operational space technology for global vegetation assessment. Bull Am Meteorol Soc 82(9):1949–1964

Kriegler FJ, Malila WA, Nalepka RF, Richardson W (1969) Preprocessing transformations and their effects on multispectral recognition. In: Proceedings of the sixth international symposium on remote sensing of environment, pp 97–131

Li X (2001) Estimation of evaporation with remote sensing in the Urumqi River Basin. M.Sc. thesis, IHE, Delft, 84pp

McKee TB, Doesken NJ, Kleist J (1993) The relationship of drought frequency and duration to time scales. In: Proceedings of the 8th conference on applied climatology, American Meteorological Society, Anaheim, 17–22 January 1993

McKee TB, Doesken J, Kleist J (1995) Drought monitoring with multiple time scales. Paper presented at ninth conference on applied climatology, American Meteorological Society, Dallas

McVicar TR, Jupp DLB (1998) The current and potential operational uses of remote sensing to aid decisions on drought exceptional circumstances in Australia: a review. Agric Syst 57 (3):399–468

Narasimhan B, Srinivasan R (2005) Development and evaluation of Soil Moisture Deficit Index (SMDI) and Evapotranspiration Deficit Index (ETDI) for agricultural drought monitoring. Agric For Meteorol 133(1–4):69–88

Neitsch SL, Arnold JG, Kiniry JR, Williams JR, King KW (2002) Soil and water assessment tool. Theoretical documentation: Version 200. TWRI TR-191, Texas Water Resources Institute, College Station

Palmer WC (1965) Meteorological drought. Weather Bureau Research Paper No. 45, US Dept. Comm., Washington, DC, 58pp

Palmer WC (1968) Keeping track of crop moisture conditions, nationwide: the new crop moisture index. Weatherwise 21(4):156–161

Roerink GJ, Menenti M, Verhoef W (2000) Reconstructing cloud-free NDVI composites using Fourier analysis of time series. Int J Remote Sens 21:1911–1917

Rouse JW, Haas RH, Schell JA, Deering DW (1973) Monitoring vegetation systems in the Great Plains with ERTS. In: Third ERTS symposium, NASA SP-351 I, pp 309–317

Su Z (2001) A Surface Energy Balance System (SEBS) for estimation of turbulent heat fluxes from point to continental scale. In: Su Z, Jacobs C (eds) Advanced earth observation—land surface climate. Publications of the National Remote Sensing Board (BCRS), USP-2, 01-02, p 183

Su Z (2002) The Surface Energy Balance System (SEBS) for estimation of turbulent heat fluxes. Hydrol Earth Syst Sci 6(1):85–99

Su Z, Troch PA, De Troch FP (1997) Remote sensing of bare soil moisture using EMAC/ESAR data. Int J Remote Sensing 18(10):2105–2124

Su Z, Yacob A, He Y, Boogaard H, Wen J, Gao B, Roerink G, van Diepen K (2003a) Assessing relative soil moisture with remote sensing data: theory and experimental validation. Phys Chem Earth 28(1–3):89–101

Su Z, Wen J, Wan L (2003) A methodology for the retrieval of land physical parameter and actual evaporation using NOAA/AVHRR data. J Jilin Univ (Earth Sci Ed) 33(sup.):106–118

Su Z, Fernández-Prieto D, Timmermans J, Chen X, Hungershoefer K, Roebeling R, Schröder M, Schulz J, Stammes P, Wang P, Wolters E (2003a) First results of the earth observation Water Cycle Multi-mission Observation Strategy (WACMOS). Int J Appl Earth Obs Geoinf 26:270–285

Thornthwaite CW (1948) An approach toward a rational classification of climate. Geogr Rev 38:55–94

Tucker CJ (1979) Red and photographic infrared linear combinations for monitoring vegetation. Remote Sens Environ 8(2):127–150

van Hoek M (2016) Drought monitoring from space: a focus on indicators, early detection and development of a web-based integrated portal. Ph.D. thesis, Chinese Academy of Sciences, 168pp

Verhoef W (2000) Theory and software. In: Roerink GJ, Menenti M (eds) Time series of satellite data: development of new products. Publications of the National Remote Sensing Board (BCRS), NRSP-2, pp 99–33

Vicente-Serrano SM, Beguería S, López-Moreno JI (2010a) A multiscalar drought index sensitive to global warming: the standardized precipitation evapotranspiration index. J Clim 23 (7):1696–1718

Vicente-Serrano SM et al (2010b) A new global 0.5 gridded dataset (1901–2006) of a multiscalar drought index: comparison with current drought index datasets based on the Palmer Drought Severity Index. J Hydrometeorol 11(4):1033–1043

Zargar Z, Sadiq R, Naser B, Khan FI (2011) A review of drought indices. Environ Rev 19:333–349